Epaxial and Limb Muscle Activity During Swimming and Terrestrial Stepping in the Adult Newt, *Pleurodeles waltl*

ISABELLE DELVOLVÉ, TIAZA BEM, AND JEAN-MARIE CABELGUEN
Laboratoire de Neurobiologie et Physiologie Comparées, Université Bordeaux I and Centre National de la Recherche Scientifique, 33120 Arcachon, France

Delvolvé, Isabelle, Tiaza Bem, and Jean-Marie Cabelguen. Epaxial and limb muscle activity during swimming and terrestrial stepping in the adult newt, *Pleurodeles waltl. J. Neurophysiol.* 78: 638–650, 1997. We have investigated the patterns of activation of epaxial musculature during both swimming and overground stepping in an adult newt (*Pleurodeles waltl*) with the use of electromyographic (EMG) recordings from different sites of the myomeric muscle dorsalis trunci along the body axis. The locomotor patterns of some limb muscles have also been investigated. During swimming, the epaxial myomeres are rhythmically active, with a strict alternation between opposite myomeres located at the same longitudinal site. The pattern of intersegmental coordination consists of three successively initiated waves of EMG activity passing posteriorly along the anterior trunk, the midtrunk, and the posterior trunk, respectively. Swimming is also characterized by a tonic activation of forelimb (dorsalis scapulae and extensor ulnae) and hindlimb (puboischiotibialis and puboischiofemoralis internus) muscles and a rhythmic activation of muscles (latissimus dorsi and caudofemoralis) acting both on limb and body axis. The latter matched the activation pattern of epaxial myomeres at the similar vertebral level. During overground stepping, the midtrunk myomeres express single synchronous bursts whereas the myomeres of the anterior trunk and those of the posterior trunk display a double bursting pattern in the form of two waves of EMG activity propagating in opposite directions. During overground stepping, the limb muscles and muscles acting on both limb and body axis were found to be rhythmically active and usually displayed a double bursting pattern. The main conclusion of this investigation is that the patterns of intersegmental coordination during both swimming and overground stepping in the adult newt are related to the presence of limbs and that they can be considered as hybrid lampreylike patterns. Thus it is hypothesized that, in newt, a chain of coupled segmental oscillatory networks, similar to that which constitutes the central pattern generator (CPG) for swimming in the lamprey, can account for both trunk motor patterns if it is influenced by limb CPGs in a way depending on the locomotor mode. During swimming, the segmental networks located close to the girdles receive extra tonic excitation coming from the limb CPGs, whereas during stepping, the axial CPGs are entrained to some extent by the limb oscillators.

INTRODUCTION

Axial movements during aquatic or terrestrial locomotion in lower vertebrates consist primarily of rhythmic lateral bending of the trunk and tail. The neural networks generating the rhythmic contractions of axial muscles that underlie lateral bending during swimming have been extensively investigated in the lamprey (reviewed in Grillner et al. 1995) and *Xenopus* tadpole (Roberts et al. 1986). By contrast, the neural circuits producing lateral bending during terrestrial locomotion in lower tetrapods have not been studied directly. Consequently, any attempt to compare and contrast the central neural circuits controlling the axial motor system during swimming and stepping has not been performed.

Among lower vertebrates, the adult newt is a suitable experimental model for investigating neural networks that generate the rhythmic contractions of axial musculature during swimming and overground stepping, because this animal can spontaneously exhibit these two locomotor modes. Furthermore, the brain stem–spinal cord of newt can be isolated in vitro and used to investigate neural networks at a cellular level (Wheatley et al. 1992). However, an essential prerequisite for an accurate identification and characterization of in vitro axial locomotor patterns is a detailed knowledge of the patterns of activation of axial muscles during locomotor movements in the intact animal.

To date, two studies have attempted to characterize the patterns of activation of axial muscles during locomotion in intact salamanders. In the first study, the epaxial musculature of *Ambystoma tigrinum* was shown to exhibit two distinct rhythmic patterns of electromyographic (EMG) activity: a rostrocaudally traveling wave of muscle contractions during swimming and a standing wave of muscle contractions during treadmill trotting (Frolich and Biewener 1992). These waves of EMG activity have been related to the lateral undulations of the body observed in kinematic studies (Ashley-Ross 1994; Daan and Belterman 1968; Frolich and Biewener 1992; Roos 1964). In the second study, the contribution of hypaxial musculature to lateral bending in *Dicampton ensatus* has been investigated (Carrier 1993). However, in both studies, EMG recordings were made only from a few longitudinal sites and, although some general features of the motor patterns during the two locomotor modes were described, we still lack a precise description of the timing of axial muscle activity along the entire body axis.

Therefore, in an attempt to provide the basis for further in vitro experiments on the neural control of tetrapod motor systems during locomotion, we have performed a detailed analysis of the EMG pattern of the axial musculature along the body axis during swimming and overground stepping in an adult newt (*Pleurodeles waltl*). We focused on epaxial musculature because it is the component of the axial musculature that produces lateral bending during both stepping and swimming (Carrier 1993). Moreover, in an attempt to relate neural circuits controlling axial movements and those controlling limb movements, we have also examined the EMG pattern of some limb muscles during the two modes of locomotion.

0022-3077/97 $5.00

METHODS

Experiments were performed on 18 fully metamorphosed amphibian urodeles (*P. waltl*) with snout vent lengths (SVLs) ranging from 78 to 102 mm. All the animals were obtained from Centre de Biologie du Développement (CNRS UMR 9925, France) and kept in an aquaria at the room temperature. No locomotor training was performed before experiments.

EMG electrode implantation

EMG electrode implantation was performed while the animal was under general anesthesia induced by immersion in a 0.1% aqueous solution of tricaine methanesulfonate. Under a dissecting microscope, pairs of fine 70-μm insulated stainless steel wires with bared ends (exposure 0.5 mm) were inserted 3–4 mm relative to the dorsal midline through small skin incisions into myomeres (2–4 electrode pairs in each animal) of the muscle dorsalis trunci. The electrode tips were separated by ~1.0 mm and the insulated portions of the wires proximal to the tips were glued to the skin overlying the dorsalis trunci muscle with cyanoacrylate adhesive. The electrode location was verified by inducing muscle contraction with electrical stimulation via the same wires and by dissection at the end of the recording session. The rostrocaudal position of the recording electrodes was expressed as fraction of the SVL. In each experiment the activity in the myomere located at 0.60 SVL level on the right side of the animal (''0.60 SVL myomere'') was recorded as the reference point in the locomotor cycle (see below).

In some experiments ($n = 5$), the latissimus dorsi or the caudofemoralis muscle was implanted to study EMG patterns of muscles acting both on the body axis and on the limbs during swimming and overground stepping. In these experiments, the forelimb muscles dorsalis scapulae and extensor ulnae and the hindlimb muscles puboischiotibialis and puboischiofemoralis internus were implanted to monitor the step cycle (Ashley-Ross 1995; Székely et al. 1969). The muscles were identified according to Francis (1934).

All electrode wire pairs were then gathered to make a light and flexible cable (length ~1 m) that was sutured to the skin of the animal's back. Sufficient slack was provided along implantation sites and points of attachment on the back so that the newt could move in an unimpeded fashion.

Protocol

After electrodes had been implanted, animals were placed in a tank (80 × 13 cm) filled with 10 cm of tap water and allowed to recover from anesthesia for 1–2 h. After recovery, the newts were easily induced to swim the length of the tank or to walk on a wet, stainless steel surface by touching or gently squeezing the base of the tail. A wet walking surface was used because the locomotor movements of the newt are smooth and continuous under these conditions (Roos 1964). The swimming episodes were sometimes preceded by a period of low-speed paddling by the limbs (see Fig. 1*A*). This mode of aquatic locomotion has not been analyzed in the present study. Immediately after each experiment, animals were killed by overanesthesia.

Data collection and analysis

The voltage signals from electrodes were differentially amplified 10,000 times (band pass 0.3–10 kHz with a 50-Hz notch filter), displayed on an oscilloscope, and stored on a eight-channel data recorder (DAT Biologic). Thereafter the data were played back on a multichannel electrostatic printer (Gould Recorder ES-1000). The EMGs from those sections of data obtained during episodes of steady locomotion were sampled (1 kHz per channel) with the use of an A-D converter (Cambridge Electronic Design 1401). The digital EMGs were full-wave rectified and smoothed by a software filter (<100 Hz). An interactive software was then used to mark manually with a cursor (resolution < 1 ms) the onset and cessation of bursts of EMG activity. The criterion used for delineation of a single EMG burst was a signal-to-noise ratio of ≥2:1 and a time separation from other bursts >20 ms.

The locomotor cycle was arbitrarily defined as the interval between the onset of two successive bursts in the right 0.60 SVL myomere. For each step cycle analyzed, the beginning (cf. ''delay'' in Fig. 4) and end of bursts of the recorded muscles were calculated with respect to the onset of the burst in the right 0.60 SVL myomere.

The data from different experiments were pooled for each locomotor mode and processed with the use of standard statistical analyses (SigmaStat software). For swimming, the mean values of the cycle duration and the mean values of the duration, the delay, and the phase lag (i.e., delay/cycle duration) of epaxial EMG bursts were calculated for each recorded site in different ranges of cycle duration (Table 1). The mean values of the phase lag between two adjacent trunk sites were compared with the use of the *t*-test (*P* values in Table 1). The dependency of both the delay and the phase lag on the cycle duration at each recorded site was tested with the use of linear regression analysis (*P* values in Table 2). For stepping, the mean values of the cycle duration and the duration and the phase lag of the EMG bursts of epaxial and limb muscles were calculated for all cycles. The slopes of the regression lines relating the phase lag of the EMG bursts with rostrocaudal position of the myomere were also calculated for both swimming and stepping. All values are presented as means ± SD.

RESULTS

General observations

As shown in Fig. 1, the EMG pattern during swimming (*A*) is characterized by a rhythmic activation of myomeres and a tonic activation of the limb muscles, whereas during stepping (*B*), myomeres and limb muscles all displayed a rhythmic activity. These differences in patterns of activation of limb muscles reflect the differences in limb movement during the two locomotor modes: during swimming the limbs are held back against the body wall, whereas they move rhythmically during stepping (cf. also Davis et al. 1990).

Figure 1 also shows that during swimming the EMG activity in tail myomeres is more pronounced than during stepping (compare activity at 1.10 SVL site in *A* and *B*), whereas the reverse occurred simultaneously in midtrunk myomeres (compare activity at 0.60 SVL site in *A* and *B*). This is consistent with the different function of tail and midtrunk during aquatic and terrestrial locomotion (Blight 1977). Another salient observation in our experiments was that the latissimus dorsi (Fig. 1) and the caudofemoralis muscles, which act both on the limb and the body axis, fired rhythmically during the two locomotor modes.

The cycle duration during swimming was consistently shorter than the cycle duration during stepping. The frequency histogram in Fig. 2, constructed from the data of a representative experiment, shows that the swimming cycle duration ranged from 350 to 625 ms (469 ± 61 ms, mean ± SE), whereas the stepping cycle duration ranged from 825 to 1,600 ms (1,138 ± 178 ms). For all 18 animals the duration of the swimming cycle ranged from 284 to 735 ms (467 ± 63 ms) and that of the stepping cycle ranged from 614 to 2,336 ms (1,111 ± 234 ms).

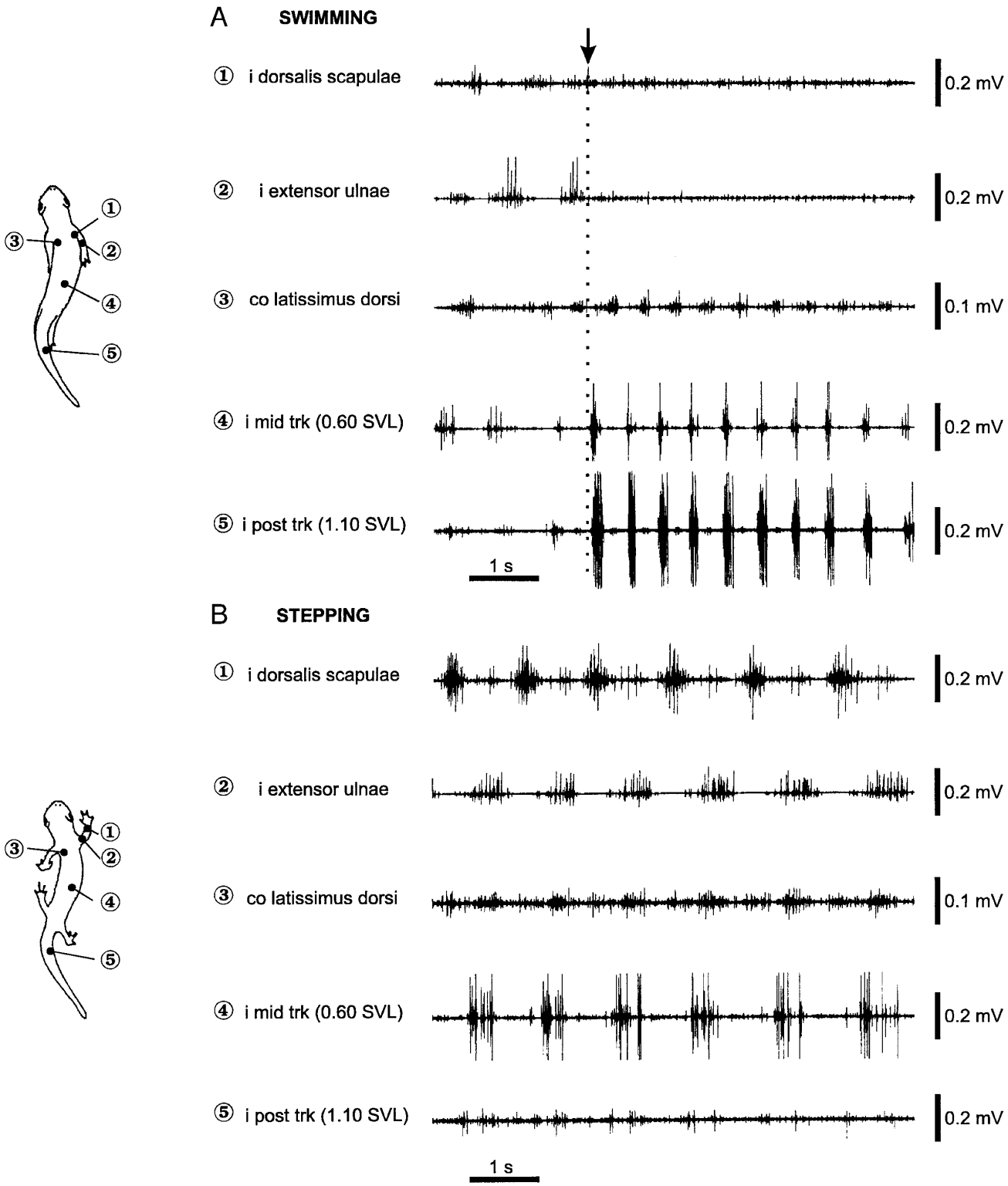

FIG. 1. Patterns of electromyographic (EMG) activity during locomotion in the newt *Pleurodeles waltl. A*: characteristic body shape of newt (*left*) and EMG recordings (*right*) during swimming. *B*: characteristic body shape of newt (*left*) and EMG recordings (*right*) during overground stepping. Two locomotor episodes were obtained from same individual a few min apart. Vertical line indicated by arrow in *A*: time at which swimming episode begins. Traces in *A* and *B*, from *top* to *bottom*, were recorded from right dorsalis scapulae, right extensor ulnae, left latissimus dorsi, midtrunk, and tail myomeres on right side of animal (see drawings at *left* and text for electrode locations). Note that for each channel, voltage amplification was identical in *A* and *B*. i, ipsilateral; co, contralateral; trk, trunk; post, posterior; SVL, snout vent length.

TABLE 1. *Characteristics of EMG activity of epaxial musculature during swimming*

Electrode Location	Cycle Duration, ms: 400–449 (427 ± 14) Burst Duration	Delay	Phase Lag	*P*	*N*	450–499 (473 ± 14) Burst Duration	Delay	Phase Lag	*P*	*N*	500–549 (521 ± 14) Burst Duration	Delay	Phase Lag	*P*	*N*
0.25	149	−82	−19.2		49	164	−90	−19.0	*	93	192	−113	−21.7	†	77
	31	*20*	*4.5*			*31*	*26*	*5.4*			*14*	*34*	*6.6*		
0.30						154	−76	−16.0	‡	17	165	−85	−16.1	‡	13
						26	*30*	*6.2*			*43*	*27*	*4.9*		
0.40						156	−4	−0.9	ns	17	148	−13	−2.3	ns	15
						31	*21*	*4.4*			*28*	*24*	*4.3*		
0.46	138	−8	−1.8		31	139	−1	−0.3	‡	47	150	9	1.6	†	17
	20	*23*	*5.2*			*25*	*18*	*3.9*			*31*	*22*	*4.2*		
0.50						103	27	5.7	ns	17	107	37	6.9	ns	15
						17	*13*	*2.6*			*20*	*25*	*4.6*		
0.51	104	16	3.8	‡	63	111	23	4.9	‡	32	125	22	4.2	†	8
	21	*14*	*3.3*			*18*	*17*	*3.7*			*31*	*20*	*3.8*		
0.55	152	−11	−2.5	‡	24	174	−9	−1.9	‡	41	176	−5	−1.0	ns	11
	19	*15*	*3.5*			*30*	*13*	*2.7*			*24*	*13*	*2.5*		
0.60	142	0	0.0	‡	400	159	0	0.0	‡	425	171	0	0.0	‡	216
	33	*0*	*0.0*			*37*	*0*	*0.0*			*40*	*0*	*0.0*		
0.74	168	26	6.1	ns	21	196	25	5.3	*	32	203	31	6.0	ns	8
	23	*12*	*3.0*			*22*	*10*	*2.2*			*21*	*12*	*2.4*		
0.76	132	23	5.4	ns	24	137	32	6.7	†	41	158	38	7.4		11
	18	*13*	*2.9*			*22*	*12*	*2.4*			*26*	*9*	*1.8*		
0.80	164	28	6.6	‡	33	183	37	8.0	‡	14					
	20	*14*	*3.3*			*16*	*13*	*2.7*							
0.85	116	11	2.6	ns	15	129	14	3.0	†	46	152	19	3.6	ns	8
	20	*15*	*3.3*			*23*	*12*	*2.4*			*30*	*14*	*2.4*		
0.90	141	13	3.1	ns	24	150	21	4.4	*	41	164	26	5.1	ns	11
	18	*10*	*2.3*			*27*	*12*	*2.6*			*29*	*15*	*3.0*		
0.95	118	13	3.0	‡	36	120	12	2.6	‡	14	140	18	3.5	†	5
	16	*9*	*2.0*			*18*	*12*	*2.6*			*20*	*8*	*1.6*		
1.00	155	44	10.4	*	67	177	54	11.5	ns	61	201	60	11.6	ns	38
	31	*15*	*3.6*			*30*	*18*	*3.8*			*26*	*29*	*5.5*		
1.10	135	51	11.8	‡	72	146	55	11.7	‡	121	153	63	12.0	‡	108
	24	*15*	*3.5*			*24*	*13*	*2.7*			*25*	*19*	*3.7*		
1.20	120	70	16.6	‡	63	134	78	16.6	‡	32	144	90	17.2	ns	8
	15	*12*	*2.8*			*16*	*16*	*3.4*			*20*	*16*	*3.0*		
1.30	153	84	19.2	‡	31	150	92	19.5	‡	47	164	96	18.4	‡	17
	67	*16*	*3.6*			*21*	*16*	*3.3*			*30*	*22*	*4.0*		
1.50	119	134	30.6		15	140	143	30.2		46	165	155	30.1		8
	37	*15*	*3.7*			*60*	*19*	*3.8*			*46*	*16*	*2.5*		

Electrode locations are given in the *1st column* as a percentage of snout vent length (SVL). For each electrode location and within each cycle duration range (400–449, 450–499, and 500–549 ms; mean ± SD indicated in parentheses) the electromyographic (EMG) burst duration (in ms), the delay of burst onset (in ms) with respect to the 0.60 SVL burst onset, and the phase lag (in percentage of cycle duration) were calculated. Means and SDs (italic) are based on *N*, number of cycles. Positive values of the delay and phase lag correspond to trunk sites activated after the 0.6 SVL myomere; negative values correspond to those activated before it. For each trunk site, the value of the phase lag was compared (*t*-test) with that of the adjacent site located caudally. Corresponding *P* values are indicated as ns ($P \geq 0.05$), * ($0.01 \leq P < 0.05$), † ($0.001 \leq P < 0.01$), and ‡ ($P < 0.001$). Note highly significant difference between phase lags of 0.51 vs. 0.55 SLV sites and between phase lags of 0.80 vs. 0.85 SVL sites. Only cycles ranging from 400 to 549 ms are presented because they were the most frequently occurring during swimming. Data are from 5 individuals.

The most common pattern of interlimb coordination during overground stepping observed in the present study was trotting or fast walking. Indeed, the histogram in Fig. 3*A* shows that the phase difference between diagonally opposed limbs expressed as a percentage of cycle duration ranged from 3.3 to 21.6% (13.8 ± 4.8%), which indicates a tendency toward an in-phase form of coordination between these limbs. In contrast, the phase difference between the two hindlimbs ranged from 37.4 to 58.4% (49.1 ± 4.3%, Fig. 3*B*), thus indicating an alternating pattern of coordination between homologous limbs.

EMG patterns in epaxial muscles during swimming

During swimming episodes, the EMG activity on the two sides of the body at the same level was strictly alternating in all animals (compare i mid trk and co mid trk in Fig. 4). Therefore in our experiments we recorded EMG activity mainly on one side of the body (usually the right side) because it reflected a similar pattern, albeit in antiphase, to the contralateral side. The mean duration of the EMG bursts calculated for several classes of cycle duration (400–550 ms) at different trunk sites ranged from 103 ± 17 to 203 ± 21 ms (Table 1), which corresponded to 21.7 ± 4.0% and 39.0 ± 4.2% of cycle duration, respectively.

Figure 4 shows that during swimming, the bursts of EMG activity at the 0.60 SVL site started after those at the 0.25 SVL site and before those at the 1.10 SVL site, indicating that a wave of EMG activity was passing rostrocaudally along the body axis of the animal. However, the rostrocaudal

TABLE 2. *Dependence of the delay and phase lag on the swimming cycle duration*

Electrode Location	Delay	Phase Lag
0.25	*	*
0.30	ns	ns
0.40	ns	ns
0.46	*	*
0.50	†	‡
0.51	†	ns
0.55	ns	ns
0.74	‡	ns
0.76	*	†
0.80	*	ns
0.85	‡	‡
0.90	*	†
0.95	ns	ns
1.00	*	ns
1.10	*	*
1.20	*	ns
1.30	*	ns
1.50	*	ns

Statistical significance of linear dependency of both delay and phase lag on the cycle duration was tested for each recorded site by use of linear regression analysis. *P* values for delay (*column 2*) and phase lag (*column 3*) are indicated as ns ($P \geq 0.05$), * ($P < 0.001$), † ($0.001 \leq P < 0.01$), and ‡ ($0.01 \leq P < 0.05$). Electrode locations are given in *column 1* as a percentage of SVL. Note that in the 3 sites located caudally to the 1.10 SVL site (i.e., in tail) the delay scaled well with the cycle duration whereas the phase lag was independent of cycle duration. Cycles ranged from 300 to 682 ms (466 ± 61 ms). Data from 5 individuals. For abbreviations, see Table 1.

order of activation of successive myomeres could be reversed at some sites of the trunk. For example, the EMG activity at 0.60 SVL site started before that of 0.50 SVL site (Fig. 5*A*) and the EMG activity in 0.90 SVL site started before that of 0.76 SVL site (Fig. 5*B*).

A detailed analysis of the delays of the onsets of bursts of EMG activity in successive myomeres (Fig. 4) revealed that the EMG wave was not propagated continuously, at a constant velocity, along the entire length of the animal. Indeed, as shown for a single individual in Fig. 6*A*, at two longitudinal sites, one located at ~0.55 SVL and the other at ~0.90 SVL, the rostrocaudal order of activation of the myomeres was actually reversed in that the caudal myomeres were activated before their more rostral neighbors (*t*-test, $P < 0.0001$ to $P < 0.05$ for different ranges of cycle duration). The same discontinuities of the rostrocaudal propagation of the EMG activity are shown in Fig. 6*B* for the data pooled from five animals (see also Table 1).

The graphs in Fig. 6, *A* and *B*, suggest that three distinct traveling waves of EMG activity were successively initiated during swimming: a first wave traveling caudally from the 0.25 SVL site to the 0.50 SVL site (i.e., along the anterior trunk); a second wave, initiated around the 0.55 SVL site and propagating posteriorly to the 0.80 SVL site (i.e., along the midtrunk), and a third wave initiated around the 0.85 SVL site and traveling down to the tip of the tail (i.e., along the posterior trunk). Figure 6*B* also shows that the delay between activations of successive myomeres located caudally to the 1.10 SVL level tended to increase with the cycle duration. The corresponding section of the graph in Fig. 6*C* suggests that the phase lag (i.e., delay/cycle duration) between those myomeres was not related to the cycle duration. A linear regression analysis confirmed that only in the caudal sites of the trunk, the delay was dependent on and the phase lag was independent of the cycle duration, whereas such was not the case in the middle and anterior trunk (Table 2).

As indicated by the graph in Fig. 6*C* and confirmed by a regression analysis, the regression line corresponding to the anterior trunk was steeper (slope: 96.4 ± 1.9% of cycle duration per SVL; $P < 0.0001$) than those corresponding to the midtrunk (slope: 35.1 ± 1.1% of cycle duration per SVL; $P < 0.0001$) and the posterior trunk (slope: 40.1 ± 0.7% of cycle duration per SVL; $P < 0.0001$). This indicates that the rostral EMG wave traveled at a slower velocity than the two more caudal counterparts.

EMG patterns in epaxial muscles during stepping

The expression of EMG activity by epaxial muscles during stepping, in contrast to swimming, varies according to the longitudinal location along the body axis (Fig. 7).

In the midtrunk (0.55–0.90 SVL) the EMG pattern within each cycle consisted of single bursts of similar duration (41.4 ± 6.8 to 43.6 ± 4.8% of cycle duration) occurring synchronously at all longitudinal locations (Figs. 7*B* and 8). However, in rostral sites of the midtrunk (0.55 SVL in Fig. 7*B*) the EMG activity envelope was maximal during the first part of the burst, whereas at more caudal sites of the midtrunk (0.90 SVL in Fig. 7*B*) maximal activity occurred during the second part of the burst.

In contrast to the relatively simple midtrunk pattern, the activity of myomeres in both anterior (0.25–0.50 SVL) and

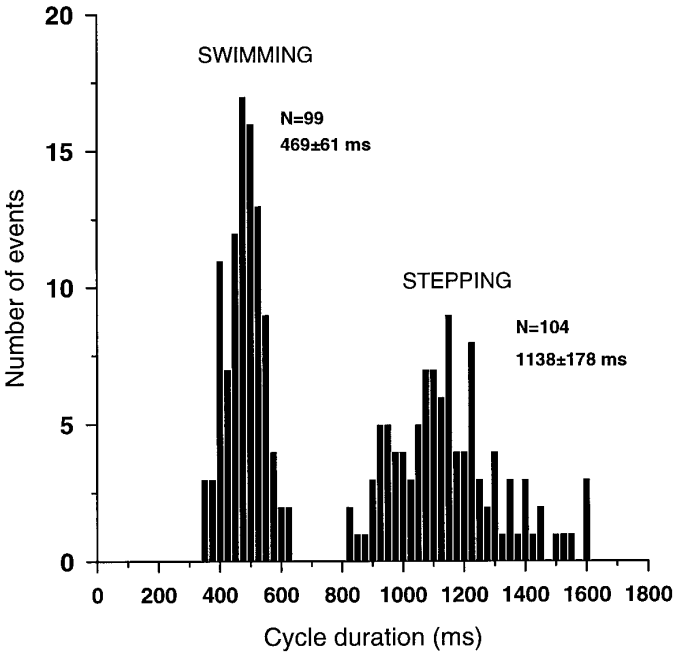

FIG. 2. Comparison of cycle duration during swimming and stepping. Each histogram plots cycle duration (abscissa, binwidth 25 ms) vs. occurrence (ordinate). Cycle duration was calculated as time interval between 2 successive EMG bursts in 0.60 SVL myomere on right side. Number of cycles (*N*) and mean ± SD are indicated to right of each histogram. Data are from same individual.

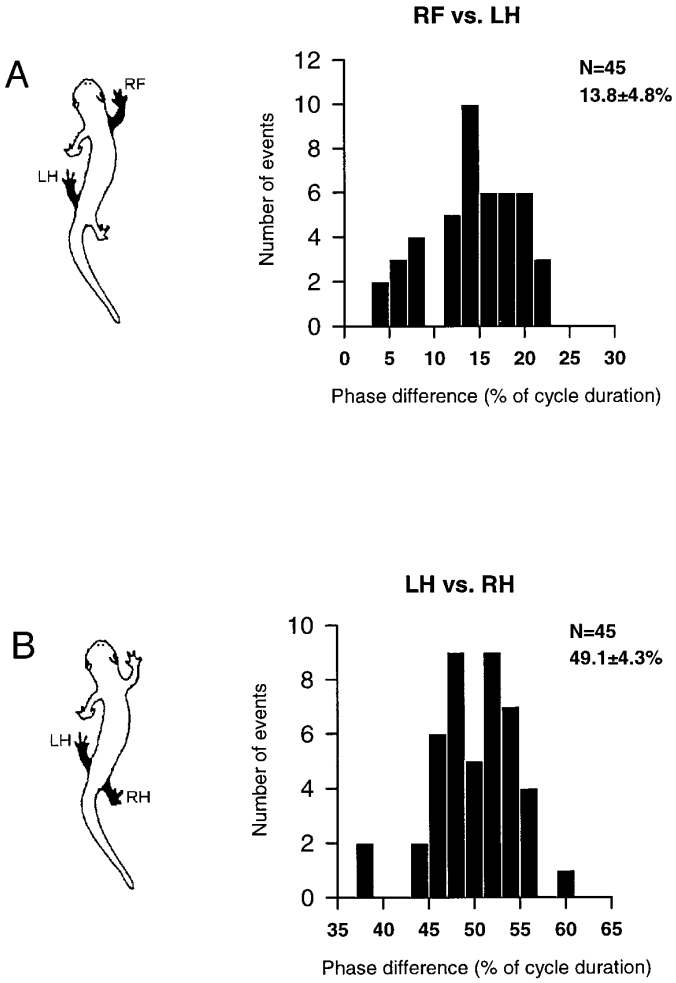

FIG. 3. Interlimb coordination during overground stepping. *A* and *B*: histograms plot phase difference between 2 limbs (shaded areas in *left insets*) on abscissa and occurrence on ordinate. In *A* (diagonally opposed limbs), phase difference, expressed as % of cycle duration, was calculated by dividing time interval between onsets of main EMG bursts (see text) of right dorsalis scapulae and left puboischiofemoralis internus by duration of step cycle. Bin width: 2% of cycle duration. In *B* (bilaterally homologous limbs), time interval between onsets of main bursts of right and left puboischiofemoralis internus was divided by duration of step cycle. Bin width: 2% of cycle duration. Number of cycles (N) and mean ± SD are indicated to right of each plot. Data are from same individual in *A* and *B*. RF, right forelimb; LH, left hindlimb; RH, right hindlimb.

posterior (1.00 SVL to tip of tail) trunk was more complex. In the anterior trunk it consisted of two bursts of EMG activity within each step cycle: one in phase and one out of phase with the midtrunk activity (cf. 0.40 SVL in Fig. 7*A* and 0.55 SVL in Fig. 7*B*). The amplitude of the ''in-phase'' burst progressively decreased in the caudorostral direction relative to that of the ''out-of-phase'' burst (cf. 0.30 SVL and 0.40 SVL in Fig. 7*A*). As shown in a summary bar diagram of EMG activity (Fig. 8), the duration of the in-phase burst was practically identical (29.4 ± 4.9% to 31.5 ± 6.4% of cycle duration) for all longitudinal positions, whereas that of the out-of-phase burst decreased significantly (42.5 ± 6.5% to 15.3 ± 4.5% of cycle duration; $P < 0.0005$) in the rostrocaudal direction.

The general features of the EMG pattern of the posterior trunk were much like the anterior trunk pattern. The posterior trunk pattern also consisted of two main bursts, again one being in phase with the midtrunk activity and the other being out of phase with it (cf. 1.10 SVL in Fig. 7*C* and 0.90 SVL in Fig. 7*B*). However, only the out-of-phase activity was clearly present in the more caudal part of the posterior trunk (1.50 SVL in Figs. 7*C* and 8). Marginally significant variations in the duration of the in-phase bursts (24.7 ± 7.1% to 26.1 ± 8.8% of cycle duration) and in that of the out-of-phase bursts (24.7 ± 7.9% to 33.3 ± 26.4% of cycle duration) did occur among recording sites.

Although the epaxial muscles displayed quite different EMG patterns during stepping and swimming, a further analysis of the timing of the EMG bursts within the step cycle also revealed propagated waves of EMG activity along the anterior trunk and the posterior trunk during stepping, which is an essential feature of swimming. Indeed, in the anterior part of the trunk, the in-phase bursts recorded from the rostral sites gradually lagged those recorded from more caudal sites, whereas a tendency for a reverse order of activation was observed for the out-of-phase bursts (compare 0.25 SVL and 0.50 SVL in Fig. 8). Similarly, along the rostral part of the posterior trunk (1.00 to 1.30 SVL) there was a progressive rostrocaudal delay in the onset of the in-phase bursts but a caudorostral delay in the onset of the out-of-phase bursts (compare 1.10 SVL and 1.30 SVL in Fig. 8). Altogether these data suggest that in both the anterior and posterior parts of the trunk, two distinct waves of EMG activity were initiated that traveled in opposite directions during each step cycle. Regression analysis revealed that the slopes of the

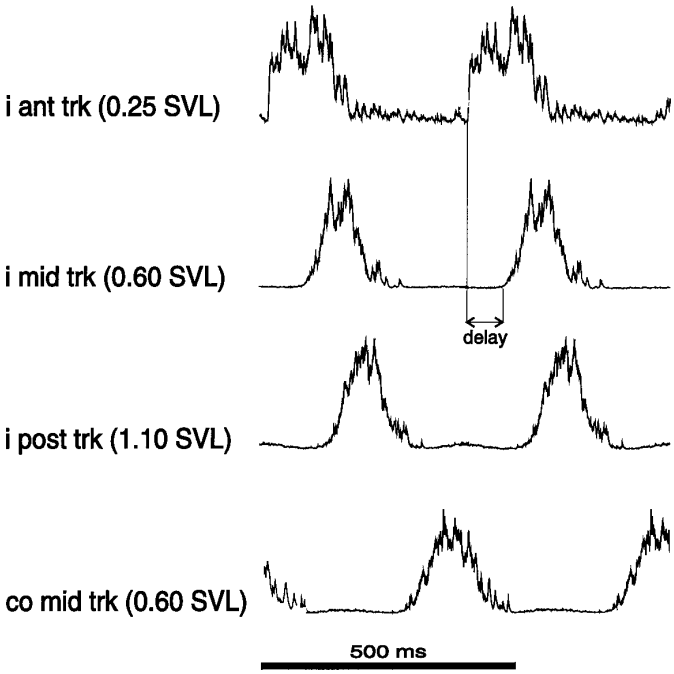

FIG. 4. EMG patterns in epaxial muscles during swimming. From *top* to *bottom*: anterior trunk (i ant trk), midtrunk (i mid trk), and posterior trunk (i post trk) myomeres on right side and midtrunk myomere on left side (co mid trk). See text for electrode locations. For each channel, EMG activity was full-wave rectified, filtered, and averaged over $n = 20–23$ consecutive swimming cycles. Averaging was triggered by onset of activity of right 0.60 SVL myomere (i mid trk). Vertical lines: time interval (''delay'') between activation of anterior trunk myomere and that of reference myomere on same side. Data are from same individual.

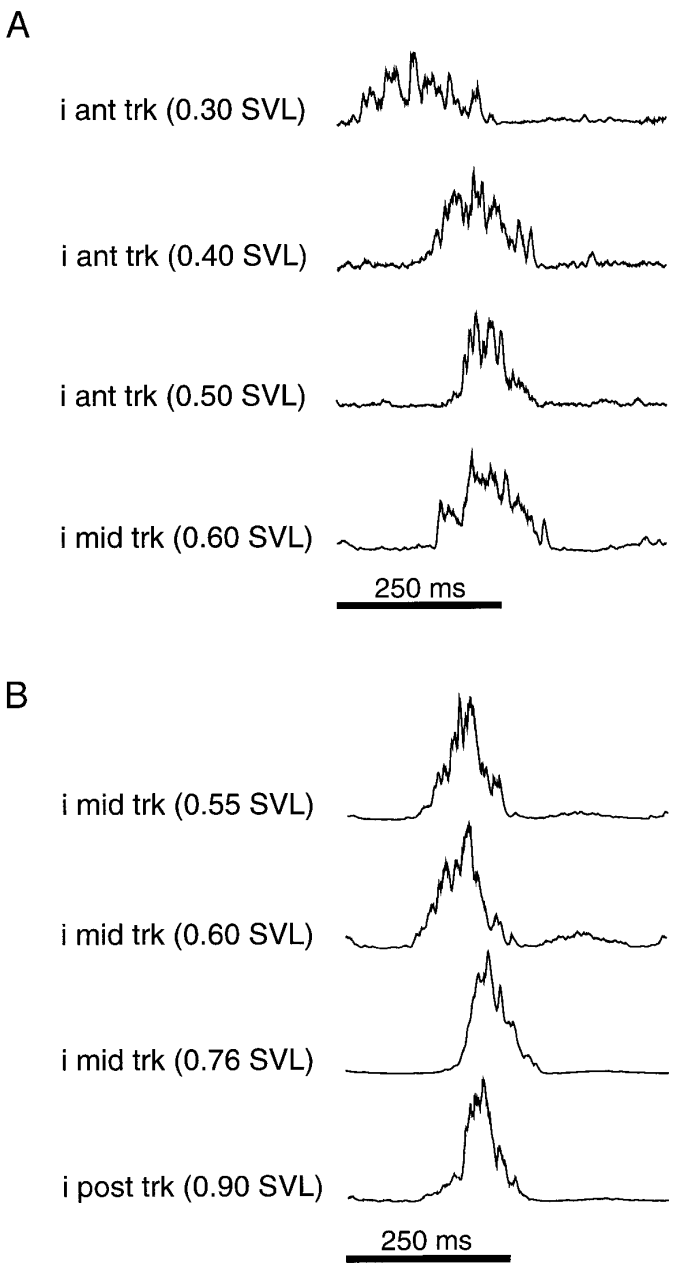

FIG. 5. EMG patterns in epaxial muscles during swimming. *A*: right anterior and midtrunk myomeres. *B*: right mid- and posterior trunk myomeres. See text for electrode locations. Conventions as in Fig. 4. Data are from 2 different swimming episodes (n = 9–20 cycles) for same individual.

regression lines corresponding to all four EMG waves were significantly different from zero ($P < 0.0001$). Moreover, the EMG waves traveling rostrocaudally in the anterior and in the posterior trunk propagated with a similar velocity, as indicated by similar values of slopes of the corresponding regression lines (+48.6 ± 9.1% and +46.3 ± 2.3% of cycle duration per SVL, respectively). On the other hand, the waves traveling caudorostrally propagated with different velocities as the slopes of the corresponding regression lines differed by a factor of ~2 (−30.6 ± 4.4% and −71.6 ± 5.7% of cycle duration per SVL for anterior and posterior trunk, respectively).

Relative timing of epaxial and limb muscle activities during swimming and stepping

The limb muscles examined in our study displayed stepping patterns that were quite similar to those reported in studies on other salamanders (Ashley-Ross 1995; Peters and Goslow 1983; Székely et al. 1969; Wheatley et al. 1992). The dorsalis scapulae, extensor ulnae, latissimus dorsi, and puboischiofemoralis internus muscles could fire two bursts within each step cycle, one that was always present (''main burst'') and the other that was not (''facultative burst''), whereas the pubioischiotibialis and caudofemoralis muscles always fired a single burst (Fig. 9, *A* and *B*).

Furthermore, our results show that during stepping, the midtrunk activity was associated with the two bursts of activity of the ipsilateral forelimb extensor ulnae (Fig. 9*A*) and with the main burst of activity of the ipsilateral hindlimb puboischiofemoralis internus (Fig. 9*B*). By contrast, the midtrunk activity alternated with the main burst of the ipsilateral forelimb dorsalis scapulae (Fig. 9*A*) and with the single burst fired by the ipsilateral hindlimb pubioischiotibialis (Fig. 9*B*).

The two muscles acting both on the limb and body axis, i.e., the latissimus dorsi in the forelimb and the caudofemoralis in the hindlimb, displayed a stepping pattern similar to that of dorsalis scapulae and pubioischiotibialis, respectively. Indeed, the pattern of latissimus dorsi consisted of two bursts within each step cycle: the facultative burst occurring during the ipsilateral 0.60 SVL activity and the main burst alternating with it (Fig. 9*A*). By contrast, the caudofemoralis fired a single burst alternating with the activity at the ipsilateral 0.60 SVL site (Fig. 9*B*). Moreover, the stepping pattern of latissimus dorsi was similar to that of ipsilateral anterior trunk myomeres (cf. 0.25 SVL in Fig. 9*A*), whereas the activity of caudofemoralis coactivated with the out-of-phase activity in ipsilateral posterior trunk myomeres (cf. 1.10 SVL in Fig. 9*B*).

As previously mentioned, during swimming the activity of the limb muscles was tonic, whereas the latissimus dorsi and the caudofemoralis fired a single burst of EMG activity within each swimming cycle (Fig. 1*A*). Figure 10 shows a bar diagram comparing the periods of EMG activity in these two muscles with those recorded at ipsilateral anterior (0.25 and 0.50 SVL), mid- (0.60 SVL), and posterior (0.90 and 1.30 SVL) trunk sites. The activity of the latissimus dorsi started after that at the 0.25 SVL site and before that at the 0.50 SVL site, whereas the caudofemoralis became active after the 0.90 SVL site and before the 1.30 SVL site.

Therefore during both swimming and stepping the activity in latissimus dorsi and caudofemoralis participates fully in the pattern of the ipsilateral anterior and ipsilateral posterior trunk, respectively.

DISCUSSION

Epaxial muscle activation

Our results demonstrate that the rhythmic activation of epaxial myomeres during swimming in adult *P. waltl* results from three temporally distinct EMG waves passing posteriorly and in succession along the length of the body. Some nonuniformity in the timing of EMG activity in epaxial mus-

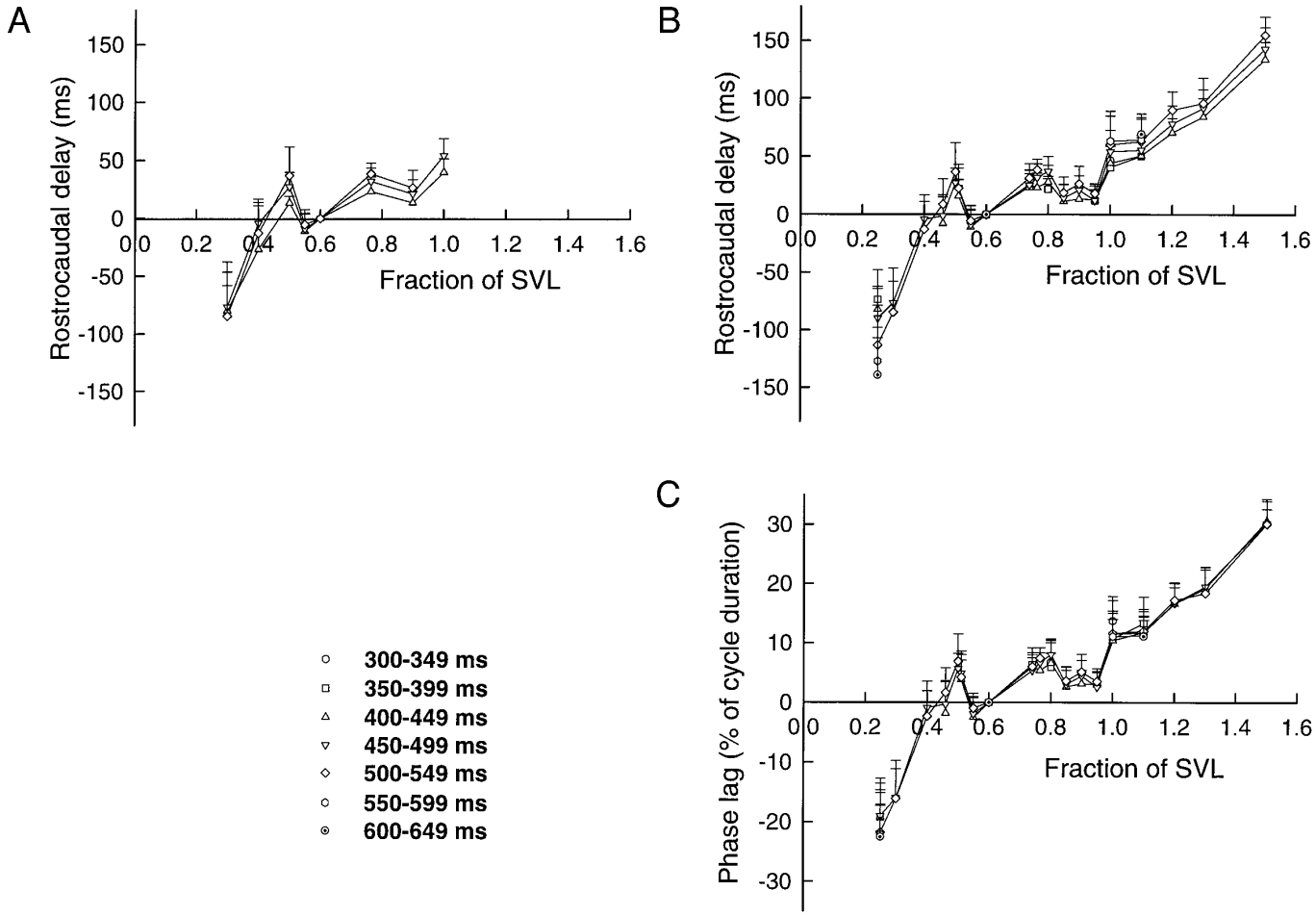

FIG. 6. Intersegmental coordination during swimming. *A* and *B*: dependence of rostrocaudal delay (ordinate) on position of myomere along body axis (abscissa). Each symbol represents mean rostrocaudal delay obtained for observed range of swimming cycle duration (indicated in *inset*). Negative values of delay: myomeres activated before reference myomere (i.e., 0.60 SVL recording site). Positive values: myomeres activated after reference myomere. *C*: dependence of rostrocaudal phase lag (ordinate) on position of myomere along body axis (abscissa). Rostrocaudal phase lag was calculated as rostrocaudal delay divided by corresponding cycle duration. Each symbol represents mean value of rostrocaudal phase lag in range of swimming cycle durations indicated in *inset.* Data were from single individual in *A* and pooled from 5 individuals in *B* and *C.* In *A–C,* vertical bars indicate SDs of delay and of phase lag, respectively.

culature during swimming in the salamander has been already reported (Frolich and Biewener 1992). The greater number of sites recorded in the present study reveals that this nonuniformity results from an actual reversal in order of activation of myomeres at two sites of the trunk (~0.55 and 0.85 SVL).

Our results further show that the speed of EMG propagation was slower in the anterior trunk than in the mid- or posterior trunk, where the speeds were comparable. In the intact trout, Williams et al. (1989) also found that the rate of EMG propagation depended on the longitudinal position, with anterior locations displaying higher speed of propagation. By contrast, in anguilliform swimmers (eel, lamprey) EMG activation appears to propagate at a constant speed (Grillner and Kashin 1976; Wallén and Williams 1984; Williams et al. 1989). These differences in the propagation velocity of EMG activity along the body could be related to the presence of limbs (urodela) or pectoral fins (trout).

Taking into account the number of body segments of *P. waltl* (7 within 0.25–0.51 SVL; 7 within 0.55–0.80 SVL; 19 within 0.85–1.50 SVL), the value of the intersegmental phase lag was 3.6, 1.3, and 1.4% of cycle duration per body segment in the anterior trunk, midtrunk, and posterior trunk, respectively. Thus the intersegemental phase lag within the caudal part of the trunk was quite similar to that previously reported in anguilliform swimmers (Grillner and Kashin 1976; Wallén and Williams 1984). In addition, our results demonstrate that the rostrocaudal delay was linearly dependent on the cycle duration and that the phase lag was independent of cycle duration (i.e., the swimming speed) only in the tail. A scaling of the delay with the cycle duration and the frequency-independent phase lag have been reported in swimming fish (Grillner 1974; Grillner and Kashin 1976; Jayne and Lauder 1995) and lamprey (Poon 1980; Wallén and Williams 1984) and are considered to be constant features of swimming behavior. From this it can be concluded that in the newt, only spinal neural circuits underlying swimming movements of the tail have all the properties of the anguilliform swimming network.

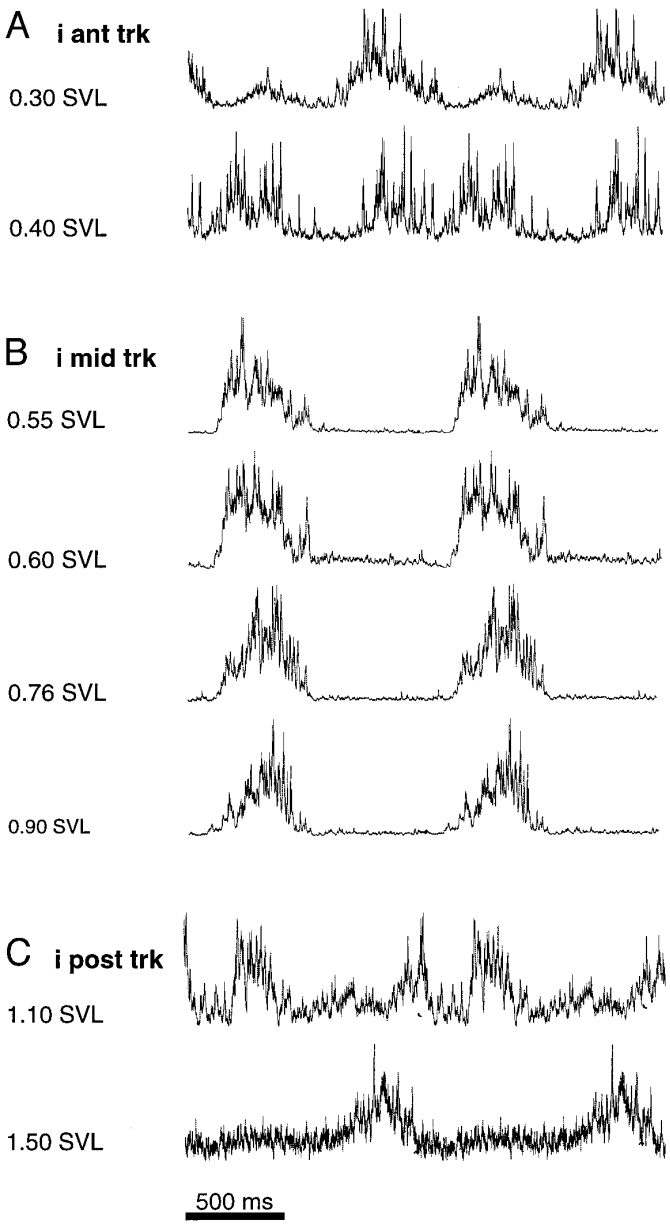

FIG. 7. EMG patterns in epaxial muscles during overground stepping. *A*: right anterior trunk myomeres. *B*: right midtrunk myomeres. *C*: right posterior trunk myomeres. See text for electrode locations. Same type of representation as in Fig. 4. Data are from same individual in *A* and *B* (n = 12 cycles) and from 2 individuals in *C* (n = 11–21 cycles).

The present study confirms that the EMG activity pattern of epaxial musculature during trotting or fast walking conforms to the one expected during lateral undulation of the trunk with fixed nodes close to the pectoral and pelvic girdles (''standing wave'') (Frolich and Biewener 1992). Indeed, the midtrunk myomeres (i.e., 0.55–0.90 SVL) were synchronously activated in alternation with the main activity in the most rostral and caudal myomeres.

Our data further show that, in contrast to midtrunk myomeres, anterior and posterior trunk myomeres exhibit a double bursting pattern during each step cycle. This activity pattern could help in maintaining the head and tail as much as possible aligned to the direction of movement by reducing, rather than actively inducing, movements of the trunk (Ashley-Ross 1994; Roos 1964). Interestingly, the additional burst in phase with midtrunk activity was more consistent for myomeres located close to the girdles (e.g., 0.40 SVL and 1.10 SVL). The role of the double activation of those myomeres might also be to control the stiffness of the trunk close to the girdles to support the action of limbs.

Limb muscle activation

During stepping, the main EMG activity of dorsalis scapulae and puboischiofemoralis internus occurs during the swing phase and that of extensor ulnae and puboischiotibialis occurs during the stance phase of the limb (Ashley-Ross 1995; Székely et al. 1969). Thus the midtrunk activity occurs during the stance phase of the ipsilateral forelimb indicated by ongoing extensor ulnae activity (Fig. 9*A*) and during the swing phase of the ipsilateral hindlimb indicated by the main burst of puboischiofemoralis internus (Fig. 9*B*). Therefore our results confirm the previous kinematic data showing that forelimb stance phase and hindlimb swing phase are related to lateral bending of the midtrunk on the same side (Ashley-Ross 1994; Daan and Belterman 1968; Roos 1964). This coordination of the limbs with the midtrunk contributes to the progress of the animal during overground stepping by

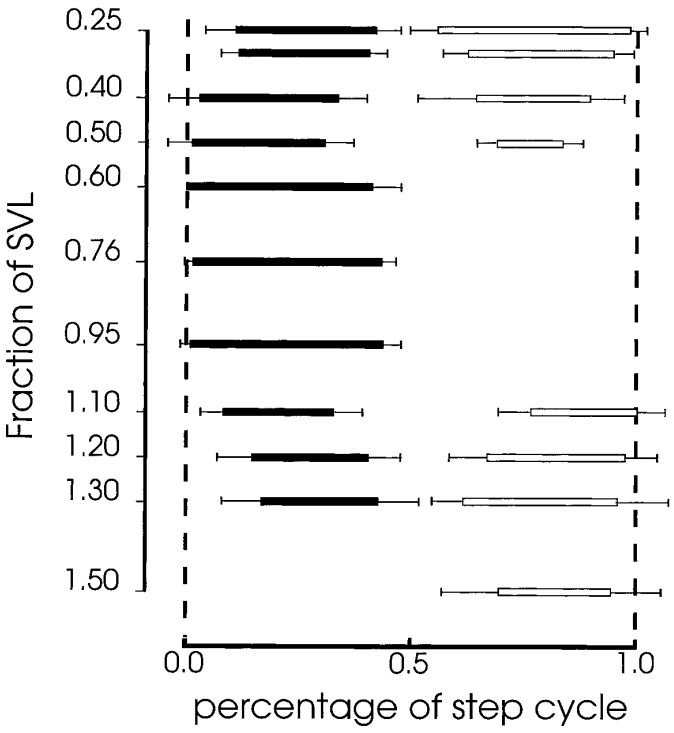

FIG. 8. Relative timing of epaxial muscle activities during step cycle. All recordings were performed on same side of body. Step cycle (abscissa) was defined as time interval between 2 successive onsets of activity in 0.60 SVL myomere. For each longitudinal location (ordinate), bars represent bursts of EMG activity expressed as percentage of step cycle. For anterior trunk and posterior trunk sites, black bars represent in-phase bursts and white bars out-of-phase bursts. Latencies of burst onset and termination were normalized to cycle duration (range: 950–1300 ms). Thin horizontal lines to left and to right of each bar: SDs of latency of burst onset and termination, respectively.

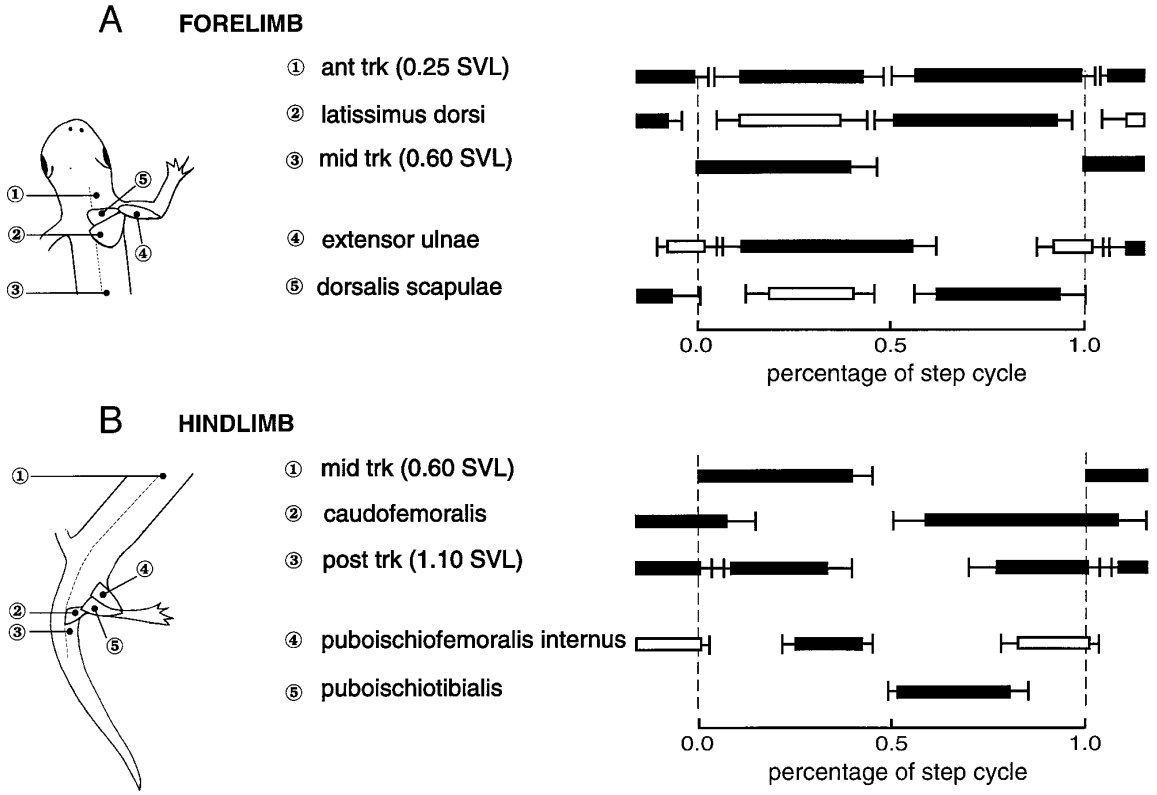

FIG. 9. Relative timing of epaxial and limb muscle activities during step cycle. Conventions as in Fig. 8. All recordings were performed on same side of body. *A*: forelimb muscles. *B*: hindlimb muscles. For limb muscles, black bars represent main bursts and white bars facultative bursts. Anatomic positions of myomeres and limb muscles are indicated in drawings at *left* (*A*, dorsal view; *B*, ventral view).

enhancing the length of the stride (Daan and Belterman 1968; Roos 1964).

In contrast to limb muscles, but similar to epaxial myomeres, the muscles acting on both the limb and body axis (i.e., latissimus dorsi and caudofemoralis) are rhythmically active during both swimming and stepping. Our results further reveal that the locomotor patterns of latissimus dorsi and caudofemoralis muscles are quite similar to those of epaxial myomeres located in the anterior trunk and in the posterior trunk, respectively. Altogether, these data strongly suggest that during swimming the motoneurons of limbic latissimus dorsi and caudofemoralis muscles are driven by the same neural networks that drive epaxial muscle activation. However, our results do not allow us to infer whether during stepping the latissimus dorsi and caudofemoralis motoneurons are still driven by the epaxial neural networks or by the neural networks that now underlie limb muscle activation.

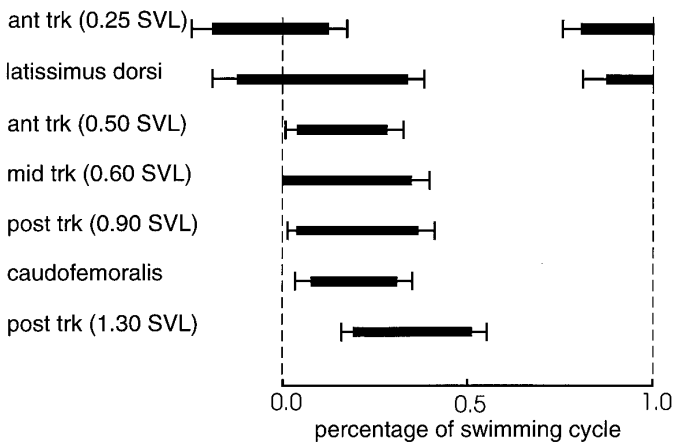

FIG. 10. Relative timing of latissimus dorsi, caudofemoralis, and epaxial muscle activities during swimming cycle. All EMG recordings were performed on same side of body. Conventions as in Fig. 9. Cycle range: 400–500 ms. Bars corresponding to latissimus dorsi and caudofemoralis are illustrated according to location of their insertions along trunk (Ashley-Ross 1992; Francis 1934).

The rhythmic activation of latissimus dorsi and caudofemoralis during swimming could play an important role in holding the limbs against the body while generating rhythmic lateral forces in time with the rhythmic movements of the trunk itself. The function of caudofemoralis during stepping has previously been discussed by others (Ashley-Ross 1995; Peters and Goslow 1983). The main burst of latissimus dorsi would assist in lifting up the forelimb during the flexor phase, whereas its facultative burst would contribute in drawing the forelimb backward during the propulsive phase (see Cabelguen et al. 1981).

Neural mechanisms of intersegmental coordination

Our results do not allow direct inferences regarding the structure of neural networks underlying the patterns of muscle activation during swimming and stepping in the newt. However, it has previously been shown in a variety of vertebrates that the major features of the EMG pattern during

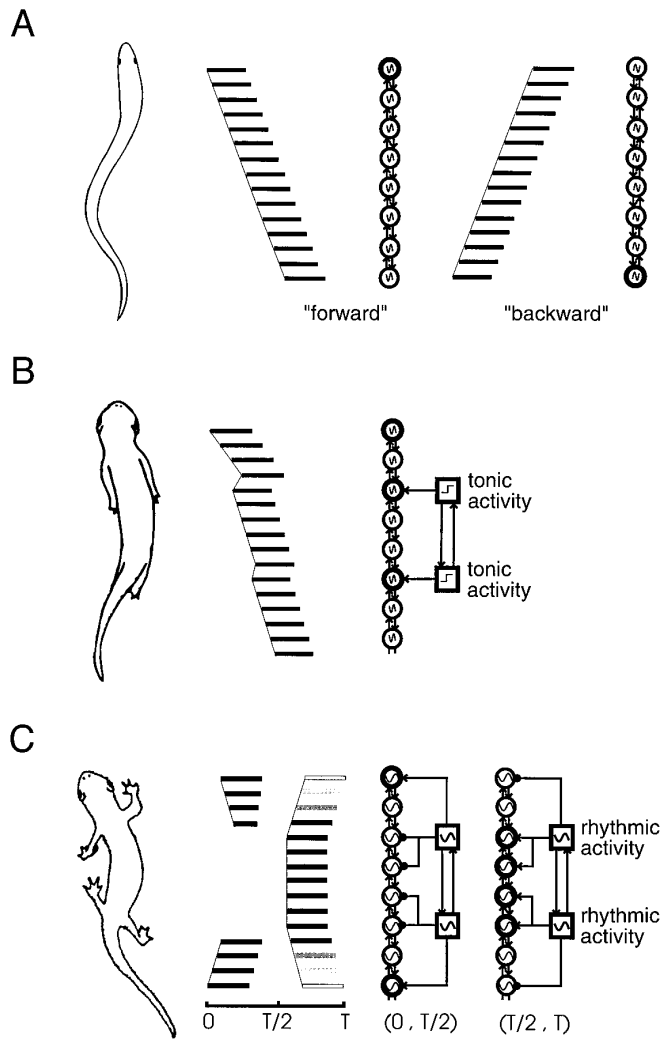

FIG. 11. Schematic diagrams of neural mechanisms of intersegmental coordination during swimming in lamprey (*A*) and during swimming (*B*) and stepping (*C*) in newt. *A*: schematic representation of ''trailing oscillator hypothesis'' (adapted from Grillner et al. 1993). Drawing at *left*: characteristic shape of lamprey during swimming. Bar diagrams: motor pattern along 1 side of body during forward and backward swimming. Bars indicate when myomeres are active. Wiring diagrams: chain of segmental oscillators (○) that underlies intersegmental pattern of coordination during forward and backward swimming. Oscillators are coupled with mutual excitation and inhibition (↑ ↓) and driven by ''leading oscillator'' (heavy ○) located at rostral end of chain during forward swimming and at caudal end of chain during backward swimming. *B*: proposed neural organization underlying intersegmental pattern of coordination during swimming in newt. Conventions as in *A*. Note 3 leading oscillators in chain (see text). The 2 boxes at *right* represent forelimb (*top*) and hindlimb (*bottom*) central pattern generators (CPGs) for locomotion that are tonically active during swimming. Horizontal lines: tonic excitatory inputs that come from limb CPGs and increase excitability of segmental oscillatory networks located close to pectoral and pelvic girdles. Three EMG waves are propagated posteriorly because of descending dominance of oscillators located in segments close to girdles. *C*: proposed neural mechanisms generating intersegmental pattern of coordination during stepping in newt. Motor pattern on one side of body during step cycle (0, T) is represented as in *B*. The lighter the bar, the weaker the EMG activity. Note the 2 leading oscillators during 1st half of step cycle (0, T/2) and synchronization of midtrunk oscillators during 2nd half of step cycle (T/2, T). Rhythmic inputs coming from limb CPGs increase (←) or decrease (●) excitability of other segmental oscillators.

steady locomotion in intact animals are similar to those of the electroneurographic patterns recorded during fictive locomotion in reduced or in vitro preparations (cat: Perret 1983; lamprey: Wallén and Williams 1984; fish: Fetcho and Svoboda 1993; chick: Jacobson and Hollyday 1982; tadpole: Kahn and Roberts 1982; mudpuppy: Wheatley et al. 1992). Thus it is very likely also that the patterns of activation of epaxial myomeres (intersegmental coordination) observed in the present study are essentially produced by the central pattern generators (CPGs) for locomotion.

According to the ''trailing oscillator hypothesis,'' the wave of EMG activity passing along the body axis during swimming in the lamprey is generated by a local increase in the excitatory drive onto a chain of segmental oscillatory circuits coupled by excitatory and inhibitory connections (Grillner et al. 1995; Matshushima and Grillner 1990, 1992). Segmental oscillators with a higher level of tonic excitation become the ''leading segments'' and drive, with a lag, segmental oscillatory networks in both the rostral and caudal directions. During forward swimming, the leading segments are located in the rostral part of the spinal cord and produce a wave of activity passing down the body axis (Fig. 11*A*, *left*), whereas during backward swimming they are located in the caudal part of the spinal cord and the wave of activity now travels in a caudorostral direction (Fig. 11*A*, *right*).

If we assume an equivalent segmental organization of the swimming network in the newt, three distinct leading segments must be hypothetized because three traveling waves are generated instead of one. Moreover, our results suggest that two of the leading segments are located close to each girdle (Fig. 11*B*). On this basis, therefore, an extra tonic excitation must impinge not only on the rostral segments (1st wave) but also on segments located close to the pectoral and pelvic girdles (2nd and 3rd waves). Our results further suggest that the influences of the leading segments located close to the girdles are asymmetric, because they entrain only more caudal segmental networks, suggesting a domination of descending over ascending coupling, at least between leading segments and their closest more rostral neighbors.

To date, no data are available from limbed vertebrates concerning the central organization of the neural networks that underlie the intersegmental coordination during stepping and the relationships between those networks and the limb CPGs (see, however, Koehler et al. 1984). Although the present study was not designed to address this issue, our data do suggest that, similarily to the intersegmental coordination during swimming, the intersegmental coordination during stepping in the newt is generated by neuronal networks that are basically similar to those underlying swimming in the lamprey (''lampreylike swimming CPG''). Indeed, a comparison of the pattern of activation of myomeres during stepping in the newt (Fig. 11*C*) with those during forward or backward swimming in lamprey (Fig. 11*A*) suggests that the former pattern can be considered as a hybrid lamprey pattern resulting from waves of activity initiated at different sites of the body and traveling rostrally or caudally along the body axis. In the first half of the step cycle (Fig. 11*C*, 0–T/2), two waves are generated (one, initiated in the rostral segments, propagates down the anterior trunk, and the other, initiated in the midtail segments, propagates up from the tail), whereas in the second half of the step cycle (Fig.

11*C*, T/2–T) the midtrunk activity spreads up and down the anterior trunk and posterior trunk, respectively. Thus an extra excitatory input should influence a lampreylike swimming network in a phase-dependent way: the rostral and midtail segments in the first half of the step cycle, the midtrunk segments in the second half of the step cycle.

Because overall limb muscle activity is tonic during swimming and rhythmic during stepping, the limb CPGs might, depending on the locomotor mode, be the source of tonic or rhythmic extra excitations onto the lampreylike swimming network. Additionally, rhythmic inhibitory influences onto the lampreylike swimming network should also explain the pattern of activity of epaxial muscles during stepping. Indeed, our data show that the propagation of the waves coming from the rostral and midtail segments toward the midtrunk was stopped close to the girdles. This suggests that the midtrunk segments may indeed receive inhibitory influences during this phase of the step cycle (Fig. 11*C*, 0–T/2). On the other hand, the progressive decrease in amplitude of the propagated waves associated with the coactivation of midtrunk myomeres might result from inhibitory influences on the rostral segments and on the midtail segments during that phase of the step cycle (Fig. 11*C*, T/2–T).

In conclusion, we propose that the two patterns of epaxial muscle activity observed in the newt can be generated by a lampreylike swimming network assuming that this network is influenced by the limb CPGs in a way depending on the locomotor mode. During swimming the propagation of activity is accelerated by an extra tonic excitation conveyed to the segmental networks located close to the girdles. During stepping, the swimming CPG is transformed by limb CPGs with the rhythmic excitation of the middle trunk, anterior trunk, and middle tail segments initiating waves of activity traveling up and down at different sites of the trunk. The ability of a chain of coupled oscillatory networks to be entrained above or below its intrinsic frequency from one end of the chain has been suggested both experimentally (Williams et al. 1990) and theoretically (Kopell and Ermentrout 1986, 1988; Kopell et al. 1990). However, it is still not known whether such a network can be entrained from more than one site of the chain, and this is a possibility that should be tested in further experimental and modeling studies.

We thank Drs. G. Le Masson and J. Simmers for helpful comments on the manuscript. We also thank Dr. J. Simmers. for correcting the English.

This study was supported by grants from Université Bordeaux I and Conseil Régional d'Aquitaine. I. Delvolvé received a studentship from the Ministère de l'Education Nationale, de l'Enseignement Supérieur et de la Recherche. T. Bem was supported by a stipend from France-Poland exchange program (Centre National de la Recherche Scientifique–Polish Academy of Sciences).

Present address of T. Bem: Institute of Biocybernetics and Biomedical Engineering, 02-109 Warsaw, Trojena 4, Poland.

Address for reprint requests: J. M. Cabelguen, Lab. Neurobiologie et Physiologie Comparées, Place Peyneau, 33120 Arcachon, France.

Received 3 June 1996; accepted in final form 25 March 1997.

REFERENCES

ASHLEY-ROSS, M. A. The comparative myology of the thigh and crus in the salamanders *Ambystoma tigrinum* and *Dicamptodon tenebrosus*. *J. Morphol.* 211: 147–163, 1992.

ASHLEY-ROSS, M. A. Hindlimb kinematics during terrestrial locomotion in a salamander (*Dicamptodon tenebrosus*). *J. Exp. Biol.* 193: 255–283, 1994.

ASHLEY-ROSS, M. A. Patterns of hind limb motor output during walking in the salamander *Dicamptodon tenebrosus*, with comparisons to other tetrapods. *J. Comp. Physiol.* 177: 273–285, 1995.

BLIGHT, A. R. The muscular control of vertebrate swimming movements. *Biol. Rev.* 52: 181–218, 1977.

CABELGUEN, J. M., ORSAL, D., PERRET, C., AND ZATTARA, M. Central pattern generation of forelimb and hindlimb locomotor activities in the cat. In: *Regulatory Functions of the CNS, Motion and Organization Principles*, edited by J. Szentagothai, M. Palkovits, and J. Hamori. Budapest: Akad. Kiadò, 1981, p. 199–211.

CARRIER, D. R. Activity of the hyaxial muscles during walking and swimming in the salamander *Dicamptodon ensatus*. *J. Exp. Biol.* 180: 75–83, 1993.

DAAN, S. AND BELTERMAN, T. Lateral bending in locomotion of some lower tetrapods. *Proc. Natl. Akad. Wetten. C* 71: 245–266, 1968.

DAVIS, B. M., AYERS, J. L., KORAN, L., CARLSON, J., ANDERSON, M. C., AND SIMPSON, S. B., JR. Time course of salamander spinal cord regeneration and recovery of swimming: HRP retrograde pathway tracing and kinematic analysis. *Exp. Neurol.* 108: 198–213, 1990.

FETCHO, J. R. AND SVOBODA, K. R. Fictive swimming elicited by electrical stimulation of the midbrain in goldfish. *J. Neurophysiol.* 70: 765–780, 1993.

FRANCIS, E.T.B. *The Anatomy of the Salamander*. Oxford, UK: Clarendon, 1934.

FROLICH, L. M. AND BIEWENER, A. A. Kinematic and electromyographic analysis of the functional role of the body axis during terrestrial and aquatic locomotion in the salamander *Ambystoma tigrinum*. *J. Exp. Biol.* 162: 107–130, 1992.

GRILLNER, S. On the generation of locomotion in the spinal dogfish. *Exp. Brain Res.* 20: 459–470, 1974.

GRILLNER, S., DELIAGINA, T., EKEBERG, O., EL MANIRA, A., HILL, R. H., LANSNER, A., ORLOVSKY, G. N., AND WALLÉN, P. Neural networks that co-ordinate locomotion and body orientation in lamprey. *Trends Neurosci.* 18: 270–279, 1995.

GRILLNER, S. AND KASHIN, S. On the generation and performance of swimming in fish. In: *Neural Control of Locomotion*, edited by R. Herman, S. Grillner, P.S.G. Stein, and D. G. Stuart. New York: Plenum, 1976, p. 181–201.

GRILLNER, S., MATSHUSHIMA, T., WADDEN, T., TEGNÉR, J., EL MANIRA, A., AND WALLÉN, P. The neurophysiological bases of undulatory locomotion in vertebrates. *Semin. Neurosci.* 5: 17–27, 1993.

JACOBSON, R. D. AND HOLLYDAY, M. Electrically evoked walking and fictive locomotion in the chick. *J. Neurophysiol.* 48: 257–270, 1982.

JAYNE, B. C. AND LAUDER, G. V. Red muscle motor patterns during steady swimming in largemouth bass: effects of speed and correlations with axial kinematics. *J. Exp. Biol.* 198: 1575–1587, 1995.

KAHN, J. A. AND ROBERTS, A. The central origin of the swimming motor pattern in embryos of *Xenopus laevis*. *J. Exp. Biol.* 99: 185–196, 1982.

KOEHLER, W. J., SCHOMBURG, E. D., AND STEFFENS, H. Phasic modulation of trunk muscle efferents during fictive spinal locomotion in cats. *J. Physiol. Lond.* 353: 187–197, 1984.

KOPELL, N. AND ERMENTROUT, G. B. Symmetry and phase coupling in chains of weakly coupled oscillators. *Comm. Pure Appl. Math.* 39: 623–660, 1986.

KOPELL, N. AND ERMENTROUT, G. B. Coupled oscillators and the design of central pattern generators. *Math. Biosci.* 90: 87–109, 1988.

KOPELL, N., ERMENTROUT, G. B., AND WILLIAMS, T. L. On chains of oscillators forced at one end. *SIAM J. Appl. Math.* 51: 1397–1417, 1990.

MATSHUSHIMA, T. AND GRILLNER, S. Intersegmental co-ordination of undulatory movements—a ''trailing oscillator'' hypothesis. *Neuroreport* 1: 97–100, 1990.

MATSHUSHIMA, T. AND GRILLNER, S. Neural mechanisms of intersegmental coordination in lamprey: local excitability changes modify the phase coupling along the spinal cord. *J. Neurophysiol.* 67: 373–388, 1992.

PERRET, C. Centrally generated pattern of motoneuron activity during locomotion in the cat. In: *Neural Origin of Rhythmic Movements*, edited by A. Roberts and B. Roberts. Cambridge, UK: Cambridge Univ. Press, 1983, p. 405–422.

PETERS, S. E. AND GOSLOW, G. E. From salamanders to mammals: continuity in musculoskeletal function during locomotion. *Brain Behav. Evol.* 22: 191–197, 1983.

POON, M.L.T. Induction of swimming in lamprey by L-DOPA and amino acids. *J. Comp. Physiol.* 136: 337–344, 1980.

ROBERTS, A., SOFFE, S. R., AND DALE, N. Spinal interneurones and swim-

ming in frog embryos. In: *Neurobiology of Vertebrate Locomotion*, edited by S. Grillner, P.S.G. Stein, D. G. Stuart, H. Forssberg, and R. Herman. London: Macmillan, 1986, p. 279–306.

ROOS, P. J. Lateral bending in newt locomotion. *Proc. Natl. Akad. Wetten. C* 67: 223–232, 1964.

SZÉKELY, G., CZÉH, G., AND VÖRÖS, G. The activity pattern of limb muscles in freely moving normal and deafferented newts. *Exp. Brain Res.* 9: 53–62, 1969.

WALLÉN, P. AND WILLIAMS, T. Fictive locomotion in the lamprey spinal cord in vitro compared with swimming in the intact and spinal animal. *J. Physiol. Lond.* 347: 225–239, 1984.

WHEATLEY, M., EDAMURA, M., AND STEIN, R. B. A comparison of intact and in-vitro locomotion in an adult amphibian. *Exp. Brain Res.* 88: 609–614, 1992.

WILLIAMS, T. L., GRILLNER, S., SMOLJANINOV, V. V., WALLÉN, P., KASHIN, S., AND ROSSIGNOL, S. Locomotion in lamprey and trout: the relative timing of activation and movement. *J. Exp. Biol.* 143: 559–566, 1989.

WILLIAMS, T. L., SIGVARDT, K. A., KOPELL, N., ERMENTROUT, G. B., AND REMLER, M. P. Forcing of coupled nonlinear oscillators: studies of intersegmental coordination in the lamprey locomotor central pattern generator. *J. Neurophysiol.* 64: 862–871, 1990.